BRAIN COMMUNICATIONS

Dysmature superficial white matter microstructure in developmental focal epilepsy

Lauren M. Ostrowski,[1,2] Daniel Y. Song,[2] Emily L. Thorn,[2] Erin E. Ross,[2] Sally M. Stoyell,[2] Dhinakaran M. Chinappen,[2] Uri T. Eden,[3] Mark A. Kramer,[3] Britt C. Emerton,[4] Amy K. Morgan,[4] Steven M. Stufflebeam[5,6] and Catherine J. Chu[2,6]

Benign epilepsy with centrotemporal spikes is a common childhood epilepsy syndrome that predominantly affects boys, characterized by self-limited focal seizures arising from the perirolandic cortex and fine motor abnormalities. Concurrent with the age-specific presentation of this syndrome, the brain undergoes a developmentally choreographed sequence of white matter microstructural changes, including maturation of association u-fibres abutting the cortex. These short fibres mediate local cortico-cortical communication and provide an age-sensitive structural substrate that could support a focal disease process. To test this hypothesis, we evaluated the microstructural properties of superficial white matter in regions corresponding to u-fibres underlying the perirolandic seizure onset zone in children with this epilepsy syndrome compared with healthy controls. To verify the spatial specificity of these features, we characterized global superficial and deep white matter properties. We further evaluated the characteristics of the perirolandic white matter in relation to performance on a fine motor task, gender and abnormalities observed on EEG. Children with benign epilepsy with centrotemporal spikes ($n = 20$) and healthy controls ($n = 14$) underwent multimodal testing with high-resolution MRI including diffusion tensor imaging sequences, sleep EEG recordings and fine motor assessment. We compared white matter microstructural characteristics (axial, radial and mean diffusivity, and fractional anisotropy) between groups in each region. We found distinct abnormalities corresponding to the perirolandic u-fibre region, with increased axial, radial and mean diffusivity and fractional anisotropy values in children with epilepsy ($P = 0.039$, $P = 0.035$, $P = 0.042$ and $P = 0.017$, respectively). Increased fractional anisotropy in this region, consistent with decreased integrity of crossing sensorimotor u-fibres, correlated with inferior fine motor performance ($P = 0.029$). There were gender-specific differences in white matter microstructure in the perirolandic region; males and females with epilepsy and healthy males had higher diffusion and fractional anisotropy values than healthy females ($P \leq 0.035$ for all measures), suggesting that typical patterns of white matter development disproportionately predispose boys to this developmental epilepsy syndrome. Perirolandic white matter microstructure showed no relationship to epilepsy duration, duration seizure free, or epileptiform burden. There were no group differences in diffusivity or fractional anisotropy in superficial white matter outside of the perirolandic region. Children with epilepsy had increased radial diffusivity ($P = 0.022$) and decreased fractional anisotropy ($P = 0.027$) in deep white matter, consistent with a global delay in white matter maturation. These data provide evidence that atypical maturation of white matter microstructure is a basic feature in benign epilepsy with centrotemporal spikes and may contribute to the epilepsy, male predisposition and clinical comorbidities observed in this disorder.

1 Department of Neuroscience, Brown University, Providence, RI 02912, USA
2 Department of Neurology, Massachusetts General Hospital, Boston, MA 02114, USA
3 Department of Mathematics and Statistics, Boston University, Boston, MA 02215, USA
4 Department of Psychiatry, Massachusetts General Hospital, Boston, MA 02114, USA
5 Department of Radiology, Massachusetts General Hospital, Boston, MA 02114, USA
6 Harvard Medical School, Boston, MA 02115, USA

Received May 7, 2019. Revised May 7, 2019. Accepted May 8, 2019. Advance Access publication June 19, 2019

Correspondence to: Catherine J. Chu, MD, Department of Neurology, Massachusetts General Hospital, 175 Cambridge Street, Ste 340, Boston, MA 02114, USA
E-mail: cjchu@mgh.harvard.edu

Keywords: BECTS; DTI; u-fibre; diffusion; rolandic epilepsy

Abbreviations: AD = axial diffusivity; BECTS = Benign epilepsy with centrotemporal spikes; HC = healthy controls; DTI = diffusion tensor imaging; FA = fractional anisotropy; MD = mean diffusivity; RD = radial diffusivity

Graphical Abstract

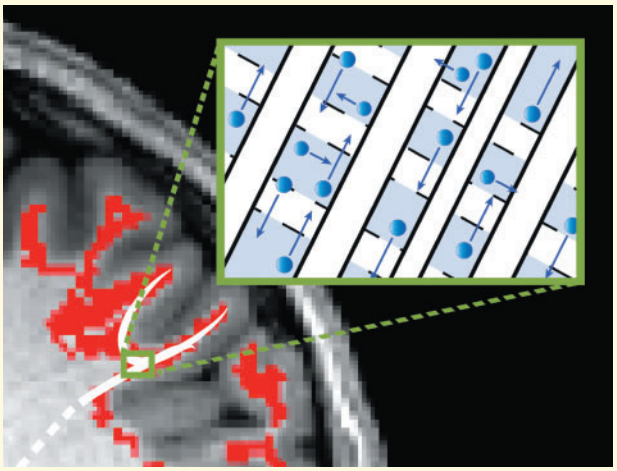

Introduction

Benign epilepsy with centrotemporal spikes (BECTS) is a common childhood epilepsy syndrome, characterized by a self-limited focal seizure disorder arising from the perirolandic cortex and fine motor abnormalities. BECTS represents 10–15% of epilepsies affecting children under the age of 15, with a 1.5:1 preponderance among males (Astradsson *et al.*, 1998; Berg *et al.*, 1999; Larsson and Eeg-Olofsson, 2006; Callenbach *et al.*, 2010; Camfield and Camfield, 2014). The majority of children experience their first seizure during elementary school years and all patients have resolution of their epilepsy by age 1616 years (Panayiotopoulos *et al.*, 2008; Callenbach *et al.*, 2010; Berg *et al.*, 2014; Camfield and Camfield, 2014). Concurrent with the age-specific presentation of this epilepsy syndrome, the brain undergoes a developmentally choreographed sequence of white matter microstructural changes across childhood and adolescence (Hagmann *et al.*, 2010; Tamnes *et al.*, 2010; Huang *et al.*, 2015; Wierenga *et al.*, 2016). Although brain developmental processes have long been favoured as fundamental to the presentation and progression of childhood epilepsy (Ben-Ari, 2006; Holmes *et al.*, 2012), the precise relationship between white matter microstructure and clinical symptoms remains poorly understood. Given the stereotyped focal presentation of BECTS, a better understanding of focal white matter microstructural features would enable identification of the anatomical substrate that supports seizure susceptibility and fine motor abnormalities in these children.

Prior work evaluating white matter abnormalities in BECTS have suggested abnormalities near the perirolandic cortex (Ciumas *et al.*, 2014; Kim *et al.*, 2014; Xiao *et al.*, 2014). These studies have relied on exploratory voxel-wise examination of the whole-brain white matter and the reported abnormalities have been complex, involving multiple fragmented subcortical regions and inconsistent findings across subjects and studies (Ciumas *et al.*, 2014; Kim *et al.*, 2014; Xiao *et al.*, 2014). Recent studies of normal white matter development have shown that local association u-fibres, including those adjoining the perirolandic cortex, mature during childhood and adolescence (Oyefiade *et al.*, 2018). As these superficial, short association fibres directly mediate local cortico-cortical communication, they provide an age-sensitive focal substrate that could support focal developmental epilepsy.

To test the relationship between focal white matter organization and disease in BECTS, we evaluated *a priori* a region of interest (ROI) corresponding to the superficial region of u-fibres underlying the seizure onset zone in children with BECTS compared with healthy control (HC) subjects. To verify the spatial specificity of these features, we evaluated superficial white matter ROIs outside of the seizure onset zone and deep white matter properties in these children. We then evaluated the abnormalities observed in the superficial perirolandic white matter in relation to fine motor performance on the

Grooved Pegboard task, gender and the cortical abnormalities observed on EEG.

Materials and methods

Subjects

All children ages 4–15 years who received a clinical diagnosis of BECTS by a child neurologist following International League Against Epilepsy criteria, including both a history of focal motor or generalized seizure and an EEG showing sleep-activated centrotemporal spikes (Berg *et al.*, 2010) were eligible for this prospective study. Subjects with a history of only a single clinical seizure were included ($n = 1$) if clinical and EEG features led to the diagnosis of BECTS (Fisher *et al.*, 2014). HC subjects without a history of seizure or known neurological or psychiatric disorder were also recruited. BECTS and HC subjects with a history of abnormal neuroimaging, autism spectrum disorder, intellectual disability or other unrelated neurological disease were excluded. Children with attention disorders and mild learning difficulties were included, as these profiles are consistent with known BECTS comorbidities (Wickens *et al.*, 2017).

A total of 25 children with BECTS were recruited; five were not able to tolerate the MRI, leaving a remaining $n = 20$ subjects with BECTS (16M, mean age ± standard deviation (SD) 11.5 ± 1.9 years). About 15 HCs were recruited; one was not able to tolerate the MRI, leaving a remaining $n = 14$ HC subjects (7M, mean age ± SD 9.8 ± 2.1 years). Medication status, date of first seizure and most recent seizure were recorded at the time of the study visit. Subject characteristics are listed in Table 1. Paediatric subjects and their guardians gave age-appropriate informed consent and this study was approved by the institutional review board at Massachusetts General Hospital.

Data acquisition

Magnetic resonance imaging

High-resolution MRI data were acquired on a 3T Magnetom Prisma scanner (Siemens, Erlangen, Germany) using a 64-channel head coil with the following sequences: diffusion tensor imaging (DTI) (64 diffusion-encoding directions, TE = 82 ms, TR = 8080 ms, flip angle = 90°, voxel size = 2.0 × 2.0 × 2.0 mm, diffusion sensitivity of b = 2000 s/mm^2, number of slices = 74, skip 0), MPRAGE (TE = 1.74 ms, TR = 2530 ms, flip angle = 7°, voxel size = 1 × 1 × 1 mm) and multi-echo FLASH (TE = 1.85, 3.85, 5.85, 7.85, 9.85, 11.85, 13.85, 15.85 ms, TR = 2000 ms, flip angle = 5°, voxel size = 1 × 1 × 1 mm). Eddy current distortion, field inhomogeneities, and head motion were corrected using FSL-FMRIB. Multi-echo Flash MPRAGE data were co-registered to the DTI data using an affine intra-subject transformation matrix generated by FreeSurfer's *bbregister* tool (Fischl, 2012).

Diffusion tensor metrics

FSL's DTIFIT was used to compute a diffusion tensor model at each voxel from which four measures, axial, radial and mean diffusivity (AD, RD and MD), and fractional anisotropy (FA), were computed (Fig. 1A–C). AD is a measure of water diffusion in the principle axis of diffusion (typically reflecting diffusion parallel to axons), and RD a measure of diffusion transverse to the principle direction (typically reflecting diffusion across axons). These measures both reflect axonal integrity, where increased AD and decreased RD signify increased fibre and myelin density (Lebel and Deoni, 2018). MD is a less specific measure and reflects overall diffusivity in all directions. FA is measure of the degree to which diffusion is directionally restricted (e.g. anisotropic). Among diffusion measures, FA is the most sensitive measure of white matter microstructural development, where increased FA suggests increased myelination and axonal coherence (Lebel and Deoni, 2018).

Electroencephalogram

Resting state EEG data were collected with a 70-channel electrode cap at a sampling rate of 2035 Hz within an average of 4.5 days from neuroimaging data collection (median 0 days, range 0–36 days). EEG data were visually inspected to remove time periods with movement, muscle and electrode artefacts, and channels containing artefact or poor recording quality were removed from analysis. EEG recordings were manually inspected by a board-certified epileptologist (C.J.C.) to identify epochs of non-REM (NREM) sleep. A minimum of 100 s of artefact-free EEG data for each patient were used (mean 184 s, range 105–200 s). The bilateral independent centrotemporal epileptiform spikes characteristic of this disease were manually marked during the NREM sleep epochs and average spike frequency per hemisphere was computed.

Neuropsychological testing

The Grooved Pegboard task was performed on each subject by a board-certified (AKM) or board-eligible (B.C.E.) neuropsychologist as close in time to the neuroimaging date as feasible (mean 28 days, range 0–142 days). This task times the placement of grooved pegs into holes, requiring that the pegs be rotated into the correct position to be successfully placed, thereby providing a quantitative evaluation of motor speed during complex sensorimotor function in the dominant and non-dominant hands.

ROI selection

To obtain subject-specific volumetric masks corresponding to the perirolandic u-fibres, pre- and post-central gyri cortical surfaces were first labelled in structural MRI space using FreeSurfer's Desikan-Killiany gyral-based atlas

Table 1 Subject characteristics

ID	Group	Gender	Age at scan (years)	Age at diagnosis (years)	Duration seizure free (mo)	ACD	Dominant hand	GPT	Comorbid neuropsychological diagnoses
1	BECTS	F	9.1	8.2	1	LEV, LTG	Right	Yes	ADHD, language + auditory processing LDs
2	BECTS	F	10.6	6.5	5	LEV	Right	Yes	Language based LD
3	BECTS	F	11.0	8.7	2	No	Right	Yes	None
4	BECTS	F	13.7	6.7	51	No	Right	Yes	ADHD
5	BECTS	M	9.0	8.3	3	No	Left	No	None
6	BECTS	M	9.1	8.3	0	No	Right	Yes	ADHD
7	BECTS	M	9.6	9.0	7	No	Right	Yes	ADHD, dyslexia
8	BECTS	M	9.8	9.7	0	OXC	Right	Yes	None
9	BECTS	M	9.9	7.7	5	No	Right	Yes	None
10	BECTS	M	10.9	8.3	10	No	Right	Yes	None
11	BECTS	M	11.3	10.8	1	No	Right	No	ADHD, LDs in written expression and mathematics
12	BECTS	M	11.5	9.7	20	No	Right	Yes	None
13	BECTS	M	11.6	10.8	3	LEV	Right	Yes	None
14	BECTS	M	11.6	10.4	14	No	Right	Yes	None
15	BECTS	M	11.8	10.1		LEV	Right	Yes	None
16	BECTS	M	11.9	7.4	24	LEV	Right	Yes	None
17	BECTS	M	13.3	9.0	26	LEV	Right	Yes	None
18	BECTS	M	14.7	10.4	1	No	Right	Yes	Dyspraxia
19	BECTS	M	14.8	7.9	40	No	Right	Yes	None
20	BECTS	M	14.9	5.9	38	No	Left	Yes	ADHD, LD in mathematics
21	HC	F	7.2				Right	Yes	None
22	HC	F	9.0				Right	Yes	None
23	HC	F	9.4				Right	Yes	None
24	HC	F	9.4				Right	No	None
25	HC	F	12.2				Left	Yes	None
26	HC	F	12.9				Right	Yes	None
27	HC	F	14.2				Right	Yes	None
28	HC	M	7.4				Right	Yes	None
29	HC	M	8.0				Unknown	No	None
30	HC	M	8.3				Right	Yes	None
31	HC	M	8.7				Right	Yes	None
32	HC	M	9.4				Right	No	None
33	HC	M	10.7				Left	Yes	None
34	HC	M	10.9				Right	Yes	None

ACD, anticonvulsant drug; GPT, grooved pegboard task; HC, healthy control; LD, learning disorder; LEV, levetiracetam; LTG, lamotrigine; OXC, oxcarbazepine; NP, neuropsychological.

(Desikan *et al.*, 2006). These labels were then projected 1 and 1.5 mm radially into white matter space. The corresponding 0.5 mm thick planar volumetric mask abutting the perirolandic region was defined as the seizure onset zone white matter label (Fig. 2). Although our goal was to select white matter adjacent to the cortical surface, we chose to ignore the 1 mm volume immediately under the grey-white boundary to reduce the possibility of including some grey matter in the label. We chose to use a 0.5 mm planar volume of white matter for our label to reduce capture of deeper white matter destined for the corona radiata. The seizure onset zone white matter masks were transformed into diffusion space using an intra-subject co-registration matrix. As the diffusion space was generated using larger $2 \times 2 \times 2$ mm voxels, to minimize capturing either grey matter or deep white matter, after co-registration with diffusion space, we chose a threshold to include only those voxels with greater than 70% overlap with the initial label in our final ROI. The resulting labels following these procedures were confirmed on visual analysis to capture the discrete region of perirolandic superficial white matter corresponding to subcortical u-fibres identified in prior diffusion studies using probabilistic tractography techniques (Oyefiade *et al.*, 2018) and in disease-specific states (Lakshmanan *et al.*, 2017). These association fibres parallel cortical folding patterns such that straight fibres in multiple orientations course around the bottom of the sulci and then embrace the cortical fold with dense terminations in the gyral tips (Zhang *et al.*, 2014).

In order to investigate superficial white matter microstructure in regions corresponding to u-fibres outside of the seizure onset zone, we used FreeSurfer's Desikan-Killiany gyral-based atlas to define cortical labels of each lobe (frontal, parietal, occipital, and temporal) in structural MRI space. We chose these labels to exclude the perirolandic region, such that the pre-central gyrus was not included in the frontal lobe, and the post-central gyrus was not included in the parietal lobe. As with the perirolandic labels, these

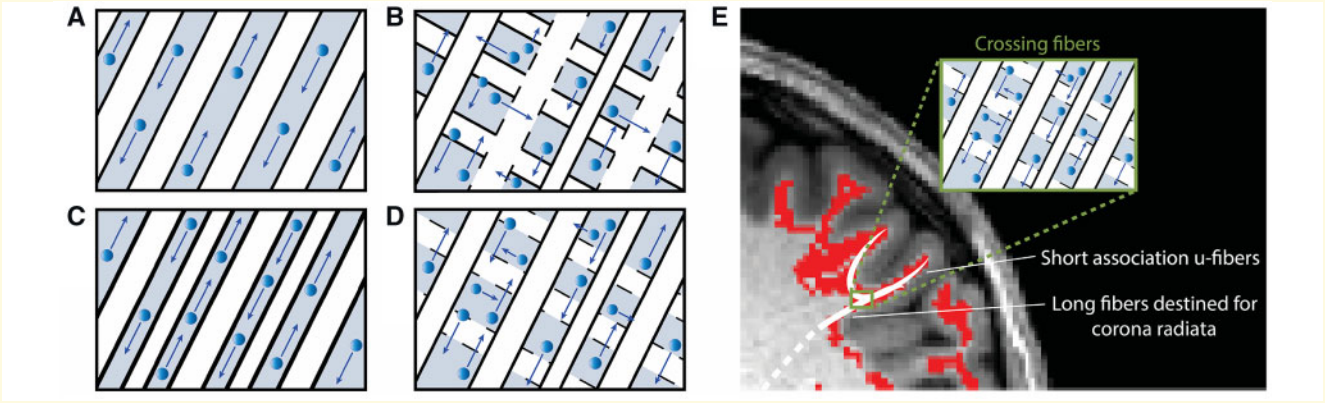

Figure 1 Relationship between white matter microstructure and high diffusion metrics. For each schematic, axons are indicated in white, myelin in black borders, interstitial space in grey and water direction and degree of diffusion by blue arrows. (**A**) AD is the degree of diffusivity in the principle direction of diffusion. Here, axial diffusivity is high due to loosely bundled myelinated axons in parallel orientation, allowing water to diffuse freely in alignment with the axonal fibres. (**B**) RD is the average diffusivity orthogonal to the direction of principle diffusion and increases with white matter de- or dysmyelination or increased crossing fibres. Here, radial diffusivity is high due to loosely bundled and weakly myelinated (signified by dotted lines) axons and crossing fibres, supporting water diffusion orthogonal to the direction that most axons are aligned. MD (not shown) is the degree of diffusion averaged across all directions, and is also high when both axial and radial diffusivity are high. (**C**) FA is a variance metric that quantifies the proportion of water diffusion in a preferred direction. Here, fractional anisotropy is high due to strong myelination and dense axonal packing, restricting water to diffuse only in alignment with the axonal fibres. (**D**) High AD, RD, MD and FA. The superficial white matter adjacent to the seizure onset zone was found to have increased axial, radial and mean diffusion in addition to increased fractional anisotropy. As this region is composed of crossing fibres, these measures most likely reflect loosely packed white matter with a dominant axonal alignment and sparse or poorly myelinated crossing fibres. (**E**) Schematic of white matter microstructure in perirolandic ROIs. The white matter immediately underneath the perirolandic cortex includes a complex mixture of crossing fibres including long-range fibres destined for the corona radiata and short-range u-fibres integrating primary sensory and motor cortices. Decreased fibre bundling or dysmyelination of the u-fibres (as in **D**) would result in increased diffusion and FA values in this region.

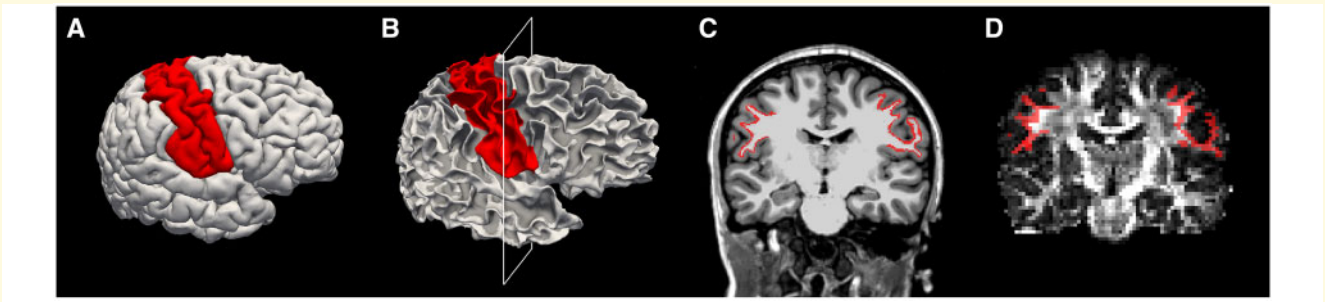

Figure 2 Example perirolandic u-fibre ROI selection process. (**A**) Pre- and post-central gyri cortical surfaces were first labelled (red) in structural MRI space using FreeSurfer's Desikan-Killiany gyral-based atlas. (**B**) The same labels (red) shown on the surface of the white matter. (**C**) The labels (red) are shown in a coronal view of a structural MRI, at the cross section identified by the white box in **B**. (**D**) To transform the labels to an appropriate volume in diffusion space, the labels were first projected radially into the white matter to capture the thin volume extending from 1 to 1.5 mm radially underlying the cortical surface. After co-registration with diffusion space, all voxels with a minimum of 70% overlap with the label were included in the final ROI. Here, an example coronal slice of the final ROI (red) is shown on a fractional anisotropy map in diffusion space.

labels were then projected 1 mm and 1.5 mm into white matter space and the corresponding 0.5 mm thick regions were used as planar volumetric masks. These masks were transformed into diffusion space using the intra-subject structural-to-diffusion co-registration matrix.

To investigate deep white matter microstructural features, whole-brain white matter masks and lobar white matter masks were generated using FreeSurfer's Desikan-Killiany white matter volumetric atlas. The masks were transformed into diffusion space using a co-registration matrix following equivalent procedures as above.

To investigate superficial white matter microstructure corresponding to the u-fibres associated with hand sensorimotor performance on the Grooved Pegboard task, we

generated a custom ROI to include the upper half of the seizure onset zone label using custom MATLAB scripts. This approach grossly captured the white matter underlying the hand sensorimotor cortex, while excluding the superficial white matter underlying the face representation area. To do this, for each subject, the midpoint between the most superior and inferior vertices in the pre-central and post-central labels in the coronal plane was calculated and a planar cut at this z-coordinate was used to segment the upper half of the perirolandic cortex. The resulting label was visually inspected to confirm that it included the 'hand knob' region. Labels were then transformed into diffusion space using a co-registration matrix as above.

Statistical analysis

For each ROI, values of the four DTI measures—AD, RD, MD, and FA—were extracted from each voxel using FMRIB's Diffusion Toolbox (Behrens *et al.*, 2003), then averaged across all voxels per ROI. Group differences (BECTS versus HCs) in DTI measures were investigated by logistic regression, with age included as an additional predictor in all analyses. For all analyses, $P < 0.05$ was used to determine significance. To address concerns that may arise from multiple comparisons across the four DTI metrics analysed (AD, RD, MD, and FA), we used the Benjamini–Hochberg procedure to control the false discovery rate (FDR), with $q = 0.05$ (Benjamini and Hochberg, 1995).

To confirm the spatial specificity of our findings, we compared the four DTI measures—AD, RD, MD, and FA—in superficial white matter outside of the perirolandic cortex and deep white matter in each lobe between groups.

We analysed the relationship between age-adjusted dominant and non-dominant hand fine motor performance and FA in the contralateral perirolandic ROIs using a linear regression model.

We were unable to account for gender in the logistic regression model due to issues of collinearity. Gender, however, is an important variable to evaluate in this disease, as males are at higher risk for BECTS than females (Bouma *et al.*, 1997). Here, we tested the relationship between gender and white matter diffusion values in three ways. Visual inspection of the data (as illustrated in Fig. 6 below) revealed a greater difference in DTI values between HC males and females compared with that observed between BECTS males and females. To quantify the difference in the male and female DTI values between HCs and BECTS, we utilized a non-parametric bootstrap resampling procedure. To do so, we first computed the empirical difference between the male and female mean DTI values found in BECTS, and that found in HCs, and then subtracted these two differences of means; the resulting statistic summarizes how the differences between the male and female DTI values differ between the BECTS and HCs. We then compared this statistic to the null hypothesis of no difference between the two groups using a resampling procedure. In this procedure, we generated surrogate data—equal in size to the original BECTS and HC data—by randomly resampling from the combined BECTS and HC data. For each resample, we computed the statistic from the surrogate data. For each DTI value, we repeated this procedure 10 000 times to generate a null distribution of values for the statistic and thereby assess the significance of the empirical result. Upon finding a significant difference between gender distributions of DTI values in BECTS and HC using the bootstrap procedure, we then compared the difference between male and female DTI values in HCs, and between male and female DTI values in children with BECTS, using two-sample *t*-tests. Finally, we confirmed group differences in DTI measures between BECTS and HCs independent of the impact of gender by comparing BECTS females and HC females using a two-sample *t*-test.

We tested the relationship between perirolandic u-fibre DTI measures to the time (months) since last known seizure prior to MRI data collection, duration of disease [measured in the time (months) from the first known seizure to the date of MRI data collection], and the intra-hemispheric spike frequency using linear regression models including age as a predictor.

Data availability

Raw data were generated at Massachusetts General Hospital and the Athinoula A. Martinos Center for Biomedical Imaging. Derived data supporting the findings of this study are available from the corresponding author on request.

Results

Distinct white matter abnormalities in the u-fibres adjacent to the seizure onset zone

To better understand the focal disease process in this developmental epilepsy syndrome, we evaluated diffusion characteristics corresponding to the region of short association u-fibres directly abutting the affected perirolandic cortex. Here, we found increased diffusivity in all diffusion metrics (AD, RD and MD) and increased FA in the BECTS subjects compared with HC ($P = 0.039$, $P = 0.035$, $P = 0.042$ and $P = 0.017$, respectively, $n = 20$ BECTS and $n = 14$ HC; all significant after correcting for multiple comparisons, see Materials and Methods section, Fig. 3). The findings of increased axial, radial and mean diffusivity are consistent with decreased axonal bundling and myelination in this region; the concurrent finding of increased fractional anisotropy is consistent with increased coherence in white matter microstructure with decreased crossing fibres in this region (Fig. 1D and E).

To evaluate the spatial specificity of the u-fibre characteristics adjacent to the seizure onset zone, we examined diffusion characteristics in the white matter abutting the

cortex outside of the seizure onset zone. We found no difference in the u-fibre microstructure underlying any of the four lobes of the brain, excluding the perirolandic seizure onset zone white matter, in any DTI measures ($P > 0.09$ for all tests, all regions). These findings demonstrate that children with BECTS have distinct microstructural abnormalities in the superficial white matter abutting the seizure onset zone, corresponding to the location of local perirolandic subcortical u-fibres.

Deep white matter microstructure is immature in BECTS

Studies evaluating global white matter maturation over childhood and adolescence have consistently demonstrated increased FA, decreased RD and inconsistent changes in MD and AD with increasing age (Hermoye *et al.*, 2006; Tamnes *et al.*, 2010). These properties reflect increased myelination, axonal coherence and fibre bundling over normal development (Budde *et al.*, 2007). To evaluate whether children with BECTS demonstrated expected white matter integrity compared with controls, we compared the diffusion characteristics for the deep white matter between BECTS and HCs. Compared with HCs, BECTS subjects had significantly decreased FA and increased RD ($P = 0.022$ and $P = 0.027$, respectively) in whole-brain white matter with no difference in MD or AD ($P > 0.15$, Fig. 4A). These results demonstrate abnormalities in average white matter integrity in children with BECTS.

To determine whether this abnormality was diffuse or localized to one region, we evaluated white matter diffusion properties by lobar region (frontal, parietal, temporal and occipital) excluding the pre- and post-central gyri. We again found significantly decreased FA and increased RD in BECTS subjects compared with HCs in each region evaluated (Fig. 4B–E). These results demonstrate that children with BECTS have abnormal white matter integrity diffusely throughout the brain. In the context of known literature on white matter development (Tamnes *et al.*, 2010), these findings are consistent with diffusely dysmature or delayed deep white matter maturation in BECTS subjects. These findings also highlight that the pattern of abnormal values observed in the perirolandic region are unique to the superficial white matter corresponding to the regions containing the subcortical u-fibres.

Perirolandic white matter FA correlates with fine motor performance

Prior work evaluating white matter microstructure and epilepsy have suggested epilepsy correlates with decreased FA, consistent with an abnormality in myelination and axonal bundling (Duncan, 2008; Madden *et al.*, 2012; Scholz *et al.*, 2013). Here, we find a unique property of increased FA locally in the white matter encasing the perirolandic gyri (Fig. 3). Because diffusion tensor imaging captures many axonal fibres per voxel, the perirolandic ROIs evaluated here include both the long-distance fibres oriented radially from the cortex and destined for the corona radiata, as well as the maturing short association u-fibres oriented parallel to the contours of the cortex (Oishi *et al.*, 2011; Zhang *et al.*, 2014). Given the crossing fibre architecture in this region, dysmature u-fibre microstructure would thus result in increased FA (Fig. 1E). U-fibres underlying the pre-central and post-central gyri are primarily involved in processing fine sensorimotor coordination. The Grooved Pegboard test assays fine motor coordination and relies on sensorimotor control and integration (Baser and Ruff, 1987; Bryden and Roy, 2005). In order to test our anatomical hypothesis that the abnormal FA we observed was related to altered u-fibre microstructure, we evaluated for an association between dominant and non-dominant hand fine motor performance and perirolandic superficial white matter FA near the hand representation area of the sensorimotor cortex in all subjects for which we had Grooved Pegboard performance scores (BECTS $n = 18$ (14M), HC $n = 11$ (6M)). Using a linear regression model, we found a negative association between FA and Grooved Pegboard performance in the perirolandic region ($P = 0.029$, Fig. 5). These results support the hypothesis that the focal abnormal DTI values present in the perirolandic cortex are related to abnormal u-fibre development and mediate fine sensorimotor performance.

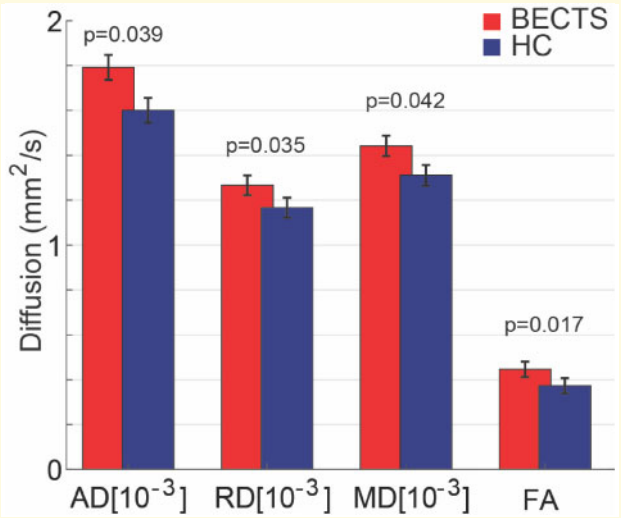

Figure 3 Perirolandic u-fibre microstructural characteristics differ in BECTS and HCs. BECTS subjects had increased diffusivity (AD, RD, MD) and FA in the white matter adjacent to the seizure onset zone compared with HCs. Bars (vertical lines) indicate mean (standard deviation) for each measure. (Note that FA is unitless.)

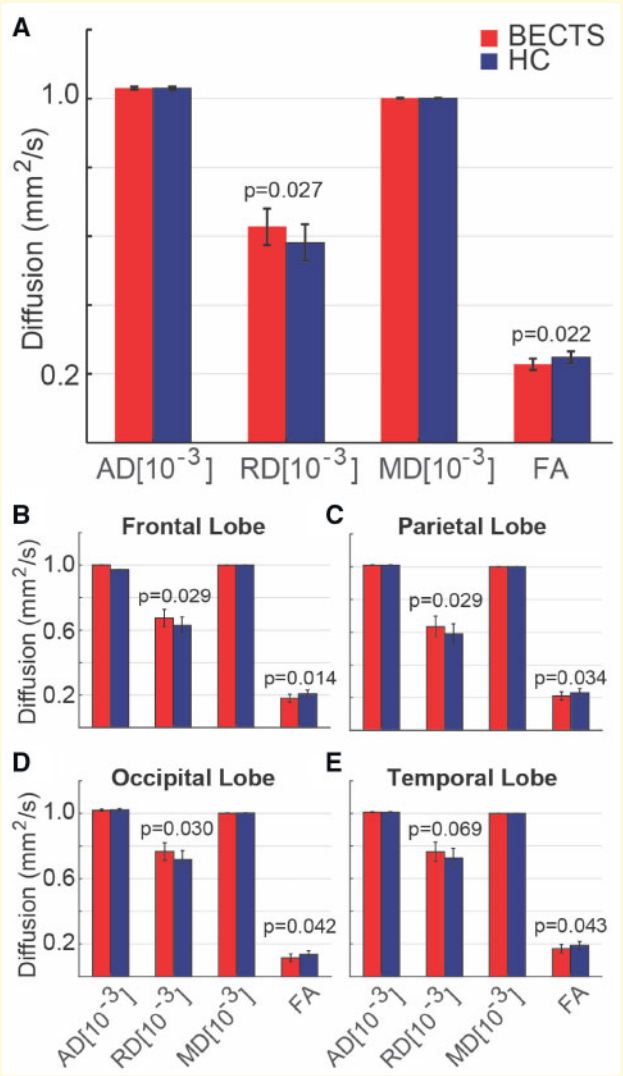

Figure 4 Whole-brain white matter microstructural characteristics differ in BECTS and HCs. (**A**) BECTS subjects had increased RD and decreased FA in whole-brain white matter, and in the white matter restricted to each brain lobe, compared with HCs [(**B**) frontal; (**C**) parietal; (**D**) occipital; (**E**) temporal lobe]. Bars (vertical lines) indicate mean (standard deviation) for each measure. (Note that FA is unitless.)

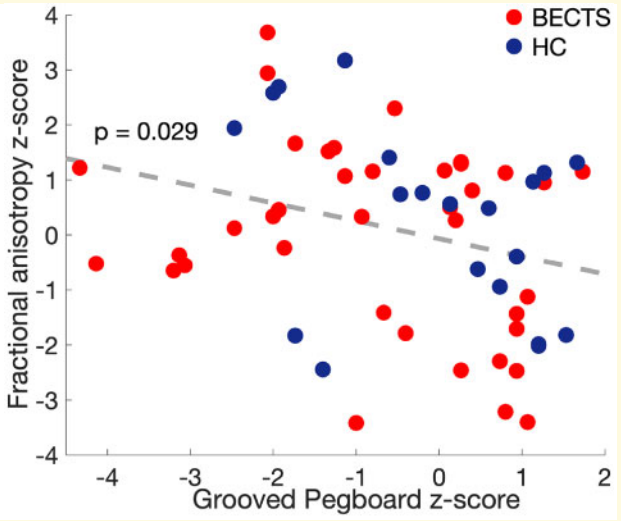

Figure 5 Higher FA values correspond with worse fine motor performance. Scatterplot of contralateral perirolandic u-fibre FA values versus groove pegboard task (GPB) performance in the dominant and non-dominant hands for all subjects (circles). A linear fit to these data (grey-dotted line) reveals a negative relationship.

Gender variability in white matter development

Visual analysis revealed increased variability in native DTI values in the perirolandic white matter among HC subjects, but high perirolandic white matter DTI values in BECTS subjects, independent of gender, consistent with a stereotyped disease process (Fig. 6A–D). This difference appeared to be at least partially explained by increased variability in DTI measures between genders in HC subjects. To test this, we performed a non-parametric bootstrap resampling analyses (see Statistical Analysis section). We found that the difference between male and female DTI values was significantly decreased in all DTI measures in the perirolandic region in BECTS subjects compared with HCs (AD $P = 0.012$; RD $P = 0.021$; MD $P = 0.014$; FA $P = 0.018$, Fig. 6E; all significant after correcting for multiple comparisons, see Materials and Methods section). Using a two-sample *t*-test (Fig. 7), we confirmed that HC females had significantly lower DTI measures than HC males in the perirolandic u-fibre ROIs in each metric measured (AD $P = 0.002$; RD $P = 0.002$; MD $P = 0.002$; FA $P = 0.035$). Conversely, we found no difference in DTI values between BECTS male and female subjects ($P > 0.4$ in all tests); rather, both male and female BECTS subjects had significantly higher DTI values than HC females ($P \leq 0.013$, for all tests, Fig. 7). These results demonstrate that in healthy children, males have higher values than females for the DTI measures considered here in the superficial white matter underlying the perirolandic cortex. However, among children with BECTS, both males and females have higher DTI values compared with female HCs, supporting a relationship between these focal microstructural abnormalities, gender and the disease process.

To determine whether the gender differences observed in the perirolandic region were unique to the seizure onset zone white matter or present diffusely in the brain, we evaluated for differences in DTI metrics between males and females in the whole-brain white matter and in the superficial white matter corresponding to subcortical u-fibres in all lobes outside of the seizure onset zone. Using a non-parametric bootstrap analysis (see Materials and Methods section), we found no difference between BECTS and HC gender distributions in whole-brain white matter metrics ($P > 0.13$ for all tests). Similarly, we found no

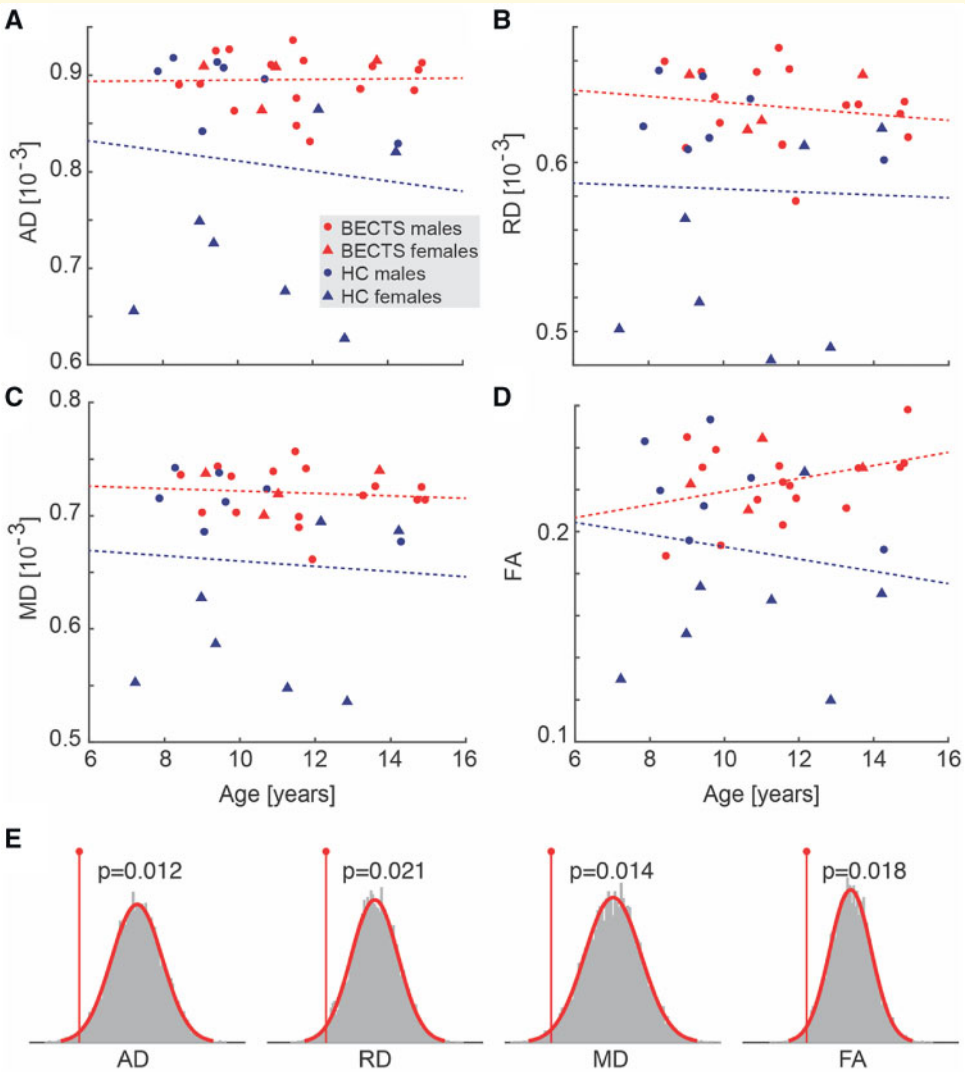

Figure 6 Gender variability in diffusion and FA values is high in HC and not BECTS subjects. (**A**–**D**) Scatterplots of raw diffusion and FA values in the perirolandic u-fibre ROIs by group and gender (see legend). Increased variability appears in HCs compared with BECTS subjects, where HC females—but not BECTS females—tend to have lower diffusion and FA values. The red (blue) lines indicate linear fits to the data from BECTS (HC) subjects. (**E**) Bootstrap distributions of group differences in gender values generated from resampled data. The empirical difference in mean gender values between BECTS and HC data is shown as a red vertical line.

difference between BECTS and HC gender values in subcortical u-fibre metrics outside of the perirolandic region ($P > 0.09$) with the exception of the temporal lobe, where increased differences in gender distributions between HCs and BECTS subjects in AD, RD and MD (but not FA) were observed ($P = 0.043$, $P = 0.038$ and $P = 0.032$, respectively), similar to differences observed in the perirolandic region. We note that although the epileptiform foci best localize to the perirolandic region, the temporal lobe is also stereotypically implicated in this focal syndrome (e.g. benign epilepsy with *centrotemporal* spikes). Thus, these results demonstrate that gender-specific differences in white matter microstructure are specific to the region corresponding to the u-fibres in the seizure onset zone. Taken together, these findings also suggest that increased diffusion and FA values in the perirolandic u-fibres are normally present in boys and may place them at increased risk of BECTS, thereby contributing to the male gender predominance of the disease.

Focal white matter microstructure does not correlate with seizure course or epileptiform spike burden

To evaluate the relationship between white matter integrity in the perirolandic region and epileptic disease in BECTS subjects, we used linear regression models (see Statistical analysis) to compare DTI measures in the perirolandic region and (i) the time from last known seizure,

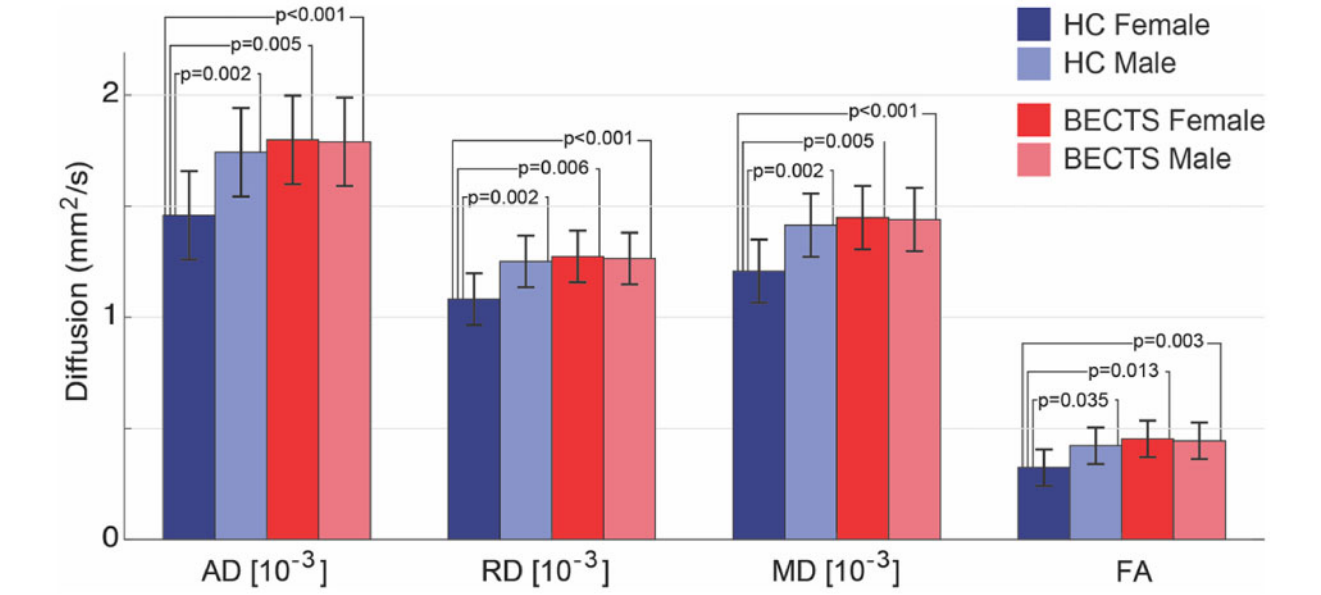

Figure 7 Diffusion and FA values differ between gender and groups. HC males have higher DTI values than HC females. BECTS males and BECTS females have higher DTI values than HC females. Bars (lines) indicate mean (standard deviation) for each measure. (Note that FA is unitless.)

(ii) the duration of epileptic disease, and (iii) spike frequency. We found no relationship between perirolandic DTI measures and any of these three measures ($P > 0.19$ for all tests).

Discussion

Several unique age-specific developmental epilepsy syndromes have been characterized (Berg *et al.*, 2010) and are postulated to relate to structural risk factors associated with normal brain maturation (Hermann *et al.*, 2002; Andersen, 2003; Overvliet *et al.*, 2013; Pardoe *et al.*, 2013; Kim *et al.*, 2015). Here, we evaluated white matter adjacent to the seizure onset zone in a common focal developmental epilepsy syndrome, BECTS, where all children have a consistent seizure onset zone localized to the perirolandic cortex. We found distinct abnormalities in the superficial white matter corresponding to the region of perirolandic u-fibres in these children. The microstructural changes observed correlate with inferior fine motor performance and reveal gender-specific differences in this gender-mediated disease. In addition, we found separate, diffuse abnormalities in deep white matter microstructure in children with BECTS compared with HCs. Together, these data provide evidence that atypical maturation of white matter microstructure is a structural feature of developmental epilepsy and may contribute to the clinical symptoms observed in this disorder.

Our findings of increased deep white matter RD and reduced FA in BECTS are consistent with prior studies in BECTS (Besseling *et al.*, 2013; Widjaja *et al.*, 2013; Ciumas *et al.*, 2014) and are consistent with a delay in the typical maturation process observed in white matter across childhood (Ashtari *et al.*, 2007; Tamnes *et al.*, 2010). Our findings of focal, superficial abnormalities in the white matter adjacent to the seizure onset zone are more prominent and specific than prior work evaluating white matter in BECTS, likely because prior work utilized whole brain and lobar voxel-wise techniques and did not focus on the microstructural white matter properties adjacent to the seizure onset zone in particular (Besseling *et al.*, 2013; Widjaja *et al.*, 2013; Ciumas *et al.*, 2014). Taken together with prior work, our findings suggest that children with BECTS have aberrant maturation of both deep white matter including long-distance fibres, as well as short association u-fibres adjacent to the seizure onset zone compared with HCs. Importantly, these findings provide evidence that childhood focal epilepsy is not simply a physiological disorder, but also involves focal structural abnormalities that can be detected using modern neuroimaging techniques.

We found that the focal white matter abnormalities present in the perirolandic region correlate with fine sensorimotor performance in children with BECTS. This result suggests that localized abnormalities in white matter maturation may contribute to the specific comorbid developmental deficiencies present in BECTS and other developmental epilepsy syndromes (Widjaja *et al.*, 2013; Kim *et al.*, 2014; Vannest *et al.*, 2015). Prior work has primarily focused on relating neurocognitive comorbidities in epilepsy to the physiological abnormalities present in children with epilepsy, such as spike rate (Xiao *et al.*, 2016), functional connectivity from EEG (van Mierlo

et al., 2014) or rhythm abnormalities (Koelewijn *et al.*, 2015; Brindley *et al.*, 2016). Our results suggest that focal abnormalities in the relevant structural association networks could be responsible for specific comorbid features present in epilepsy patients, independent of physiological features. Further, the diffusion abnormalities we observed could be consistent with a relatively dysmature white matter development process in these children and not necessarily a permanent pathological aberrant. In this case, further maturation over time would be expected to lead to disease resolution, as is observed in BECTS and other self-limited childhood epilepsy syndromes. Future, longitudinal work is required to determine whether the white matter abnormalities ultimately resolve concomitant with the fine motor difficulties observed in these children. In this cross sectional study, we did not observe a relationship between white matter microstructural features and duration seizure free, a proxy for likelihood of disease resolution, suggesting that disease resolution requires more complex compensatory mechanisms than simply resolution of transient perirolandic white matter abnormalities.

In addition to structural developmental changes in the brain, genetic contributions are expected to contribute to seizure risk in BECTS. One large study recently found that 20% of atypical BECTS cases had a mutation in the GRIN2A gene, encoding an NMDA receptor (Lesca *et al.*, 2013). However, previous work in monozygotic twins has reported complete discordance in BECTS (Vadlamudi *et al.*, 2006, 2014). Furthermore, although EEG abnormalities appear to be inherited in an autosomal dominant fashion in focal childhood epilepsy (Heijbel *et al.*, 1975; Doose, 1997), seizure risk is not, and further risk factors must therefore be contributing to the disease process. Identifying structural correlates to the disease may enable better identification of those at risk beyond genetic susceptibility. Supporting a relative genetic contribution, here, we found differences in white matter microstructure between healthy boys and girls, where boys' white matter showed less mature diffusion properties in the perirolandic region. Among children with BECTS, both boys and girls had diffusion values consistent with immature white matter, suggesting that focal, dysmature white matter in the perirolandic region may be a risk factor for BECTS, and further contribute to the male gender prevalence seen in this disease.

Notably, we did not find a relationship between white matter microstructural changes and spike rate or epilepsy course. We also found that prolonged periods of seizure freedom, corresponding to the resolution of epilepsy, did not correlate directly with the resolution of white matter microstructural abnormalities. These results suggest that although white matter maturation can be driven by cortical activity (Markham and Greenough, 2004; Bengtsson *et al.*, 2005), the white matter changes observed here are likely not directly caused by the epileptiform process. Rather, both seizures and the focal white matter changes observed could result from a shared upstream process or the white matter features could be causally upstream of the epilepsy. In the latter case, a paucity of u-fibre input could result in a disruptive relative increase in thalamocortical input to the sensorimotor cortex. It is also possible that our ROIs were not specific enough to identify a subtle relationship between white matter and epileptiform features. Here, we included white matter adjacent to the entire perirolandic cortex and corresponding to the sensorimotor features of this disease. However, the seizure onset zone in BECTS is likely constrained to the inferior portion of this cortex, near the face and hand representation areas (Huiskamp *et al.*, 2004). Studies utilizing source imaging and co-localization techniques to evaluate white matter characteristics corresponding to patient-specific epileptic foci may be better able to identify a relationship between white matter and epilepsy features.

This study reveals unique, focal abnormalities in white matter microstructure that correspond with the seizure onset zone and sensorimotor deficits in children with BECTS. These results offer new insights into the pathological process underlying focal childhood epilepsy and the relationship between white matter microstructure and a common comorbidity present in these children. Future work targeting specific white matter paths that may underlie other common neurocognitive deficits seen in children with BECTS, such as attentional and language disorders, can further clarify the relationship between cortical connectivity and epilepsy comorbidities. In addition, the relationship between white matter integrity and the seizures and abnormal cortical physiology present in these children remains poorly understood. Future studies evaluating the longitudinal changes that occur over the course of this disease may provide insight into the maturational or compensatory processes that underlie seizure risk and contribute to disease resolution. Overall, by validating the long-held intuition that focal childhood epilepsy relates to abnormalities in the maturation of structural brain networks, this work contributes to a more complete understanding of the multifaceted disease process in epilepsy.

Acknowledgements

The authors would like to thank McKenna Parnes and Grace Xiao for their assistance in MRI and EEG data collection for this project.

Funding

This work was supported by the NIH National Institute of Neurological Disorders and Stroke (NINDS; grant number K23-NS092923) and National Science Foundation Division of Mathematical Sciences (NSF DMS; grant number 1451384).

Competing interests

The authors report no competing interests.

References

Andersen SL. Trajectories of brain development: point of vulnerability or window of opportunity? Neurosci Biobehav Rev 2003; 27: 3–18.

Ashtari M, Cervellione KL, Hasan KM, Wu J, McIlree C, Kester H, et al. White matter development during late adolescence in healthy males: a cross-sectional diffusion tensor imaging study. NeuroImage 2007; 35: 501–10.

Astradsson A, Olafsson E, Ludvigsson P, Björgvinsson H, Hauser WA. Rolandic epilepsy: an incidence study in Iceland. Epilepsia 1998; 39: 884–6.

Baser CA, Ruff RM. Construct validity of the San Diego Neuropsychological Test Battery. Arch Clin Neuropsychol 1987; 2: 13–32.

Behrens TEJ, Woolrich MW, Jenkinson M, Johansen-Berg H, Nunes RG, Clare S, et al. Characterization and propagation of uncertainty in diffusion-weighted MR imaging. Magn Reson Med 2003; 50: 1077–88.

Ben-Ari Y. Basic developmental rules and their implications for epilepsy in the immature brain. Epileptic Disord 2006; 8: 91–102.

Bengtsson SL, Nagy Z, Skare S, Forsman L, Forssberg H, Ullén F. Extensive piano practicing has regionally specific effects on white matter development. Nat Neurosci 2005; 8: 1148–50.

Benjamini Y, Hochberg Y. Controlling the false discovery rate: a practical and powerful approach to multiple testing, J R Statist Soc Ser B 1995; 57: 289–300.

Berg AT, Berkovic SF, Brodie MJ, Buchhalter J, Cross JH, Van Emde Boas W, et al. Revised terminology and concepts for organization of seizures and epilepsies: report of the ILAE Commission on Classification and Terminology, 2005–2009. Epilepsia 2010; 51: 676–85.

Berg AT, Rychlik K, Levy SR, Testa FM. Complete remission of childhood-onset epilepsy: stability and prediction over two decades. Brain 2014; 137: 3213–22.

Berg AT, Shinnar S, Levy SR, Testa FM. Newly diagnosed epilepsy in children: presentation at diagnosis. Epilepsia 1999; 40: 445–52.

Besseling RM, Jansen JF, Overvliet GM, van der Kruijs SJ, Ebus SC, de Louw A, et al. Reduced structural connectivity between sensorimotor and language areas in rolandic epilepsy. PLoS One 2013; 8: e83568.

Bouma PA, Bovenkerk AC, Westendrop RG, Bruower OF. The course of benign partial epilepsy of childhood with centrotemporal spikes: a meta-analysis. Neurology 1997; 48: 430–7.

Brindley LM, Koelewijn L, Kirby A, Williams N, Thomas M, te Water-Naudé J, et al. Ipsilateral cortical motor desynchronisation is reduced in Benign Epilepsy with Centro-Temporal Spikes. Clin Neurophysiol 2016; 127: 1147–56.

Bryden PJ, Roy EA. A new method of administering the Grooved Pegboard Test: performance as a function of handedness and sex. Brain Cogn 2005; 58: 258–68.

Budde MD, Kim JH, Liang HF, Schmidt RE, Russell JH, Cross AH, et al. Toward accurate diagnosis of white matter pathology using diffusion tensor imaging. Magn Reson Med 2007; 57: 688–95.

Callenbach PM, Bouma PA, Geerts AT, Arts WF, Stroink H, Peeters EA, et al. Long term outcome of benign childhood epilepsy with centrotemporal spikes: Dutch Study of Epilepsy in Childhood. Seizure 2010; 19: 501–6.

Camfield CS, Camfield PR. Rolandic epilepsy has little effect on adult life 30 years later: a population-based study. Neurology 2014; 82: 1162–6.

Ciumas C, Saignavongs M, Ilski F, Herbillon V, Laurent A, Lothe A, et al. White matter development in children with benign childhood epilepsy with centro-temporal spikes. Brain 2014; 137: 1095–106.

Desikan RS, Ségonne F, Fischl B, Quinn BT, Dickerson BC, Blacker D, et al. An automated labeling system for subdividing the human cerebral cortex on MRI scans into gyral based regions of interest. Neuroimage 2006; 31: 968–80.

Doose H. Genetic EEG traits in the pathogenesis of the epilepsies. J Epilepsy 1997; 10: 97–110.

Duncan JS. Imaging the brain's highways—diffusion tensor imaging in epilepsy. Epilepsy Curr 2008; 8: 85–9.

Fischl B. FreeSurfer. Neuroimage 2012; 62: 774–81.

Fisher RS, Acevedo C, Arzimanoglou A, Bogacz A, Cross JH, Elger CE, et al. ILAE official report: a practical clinical definition of epilepsy. Epilepsia 2014; 55: 475–82.

Hagmann P, Sporns O, Madan N, Cammoun L, Pienaar R, Wedeen VJ, et al. White matter maturation reshapes structural connectivity in the late developing human brain. Proc Natl Acad Sci USA 2010; 107: 19067–72.

Heijbel J, Blom S, Rasmuson M. Benign epilepsy of childhood with centrotemporal EEG foci: a genetic study. Epilepsia 1975; 16: 285–93.

Hermann B, Seidenberg M, Bell B, Rutecki P, Sheth R, Ruggles K, et al. The neurodevelopmental impact of childhood-onset temporal lobe epilepsy on brain structure and function. Epilepsia 2002; 43: 1062–71.

Hermoye L, Saint-Martin C, Cosnard G, Lee SK, Kim J, Nassogne MC, et al. Pediatric diffusion tensor imaging: normal database and observation of the white matter maturation in early childhood. NeuroImage 2006; 29: 493–504.

Holmes GL, Milh MDM, Dulac O. Maturation of the human brain and epilepsy. In: Dulac O, Lassonde M, Sarnat HB, editors. Handbook of clinical neurology. Vol. 107. Radarweg: Elsevier; 2012. p. 441–6.

Huang H, Shu N, Mishra V, Jeon T, Chalak L, Wang ZJ, et al. Development of human brain structural networks through infancy and childhood. Cereb Cortex 2015; 25: 1389–404.

Huiskamp G, van Der Meij W, van Huffelen A, van Nieuwenhuizen O. High resolution spatio-temporal EEG-MEG analysis of rolandic spikes. J Clin Neurophysiol 2004; 21: 84–95.

Kim EH, Yum MS, Shim WH, Yoon HK, Lee YJ, Ko TS. Structural abnormalities in benign childhood epilepsy with centrotemporal spikes (BCECTS). Seizure 2015; 27: 40–6.

Kim SE, Lee JH, Chung HK, Lim SM, Lee HW. Alterations in white matter microstructures and cognitive dysfunctions in benign childhood epilepsy with centrotemporal spikes. Eur J Neurol 2014; 21: 708–17.

Koelewijn L, Hamandi K, Brindley LM, Brookes MJ, Routley BC, Muthukumaraswamy SD, et al. Resting-state oscillatory dynamics in sensorimotor cortex in benign epilepsy with centro-temporal spikes and typical brain development. Hum Brain Mapp 2015; 36: 3935–49.

Lakshmanan R, Adams ME, Lynch DS, Kinsella JA, Phadke R, Schott JM, et al. Redefining the phenotype of ALSP and *AARS2* mutation-related leukodystrophy. Neurol Genet 2017; 3: e135.

Larsson K, Eeg-Olofsson O. A population based study of epilepsy in children from a Swedish county. Eur J Paediatr Neurol 2006; 10: 107–13.

Lebel C, Deoni S. The development of brain white matter microstructure. Neuroimage 2018; 182: 207–18.

Lesca G, Rudolf G, Bruneau N, Lozovaya N, Labalme A, Boutry-Kryza N, et al. GRIN2A mutations in acquired epileptic aphasia and related childhood focal epilepsies and encephalopathies with speech and language dysfunction. Nat Genet 2013; 45: 1061–6.

Madden DJ, Bennett IJ, Burzynska A, Potter GG, Chen NK, Song AW. Diffusion tensor imaging of cerebral white matter integrity in cognitive aging. Biochim Biophys Acta 2012; 1822: 386–400.

Markham JA, Greenough WT. Experience-driven brain plasticity: beyond the synapse. Neuron Glia Biol 2004; 1: 351–63.

Oishi K, Huang H, Yoshioka T, Ying SH, Zee DS, Zilles K, et al. Superficially located white matter structures commonly seen in the

human and the macaque brain with diffusion tensor imaging. Brain Connect 2011; 1: 37–47.

Overvliet GM, Besseling RMH, Jansen JFA, van der Kruijs SJM, Vles JSH, Hofman PAM, et al. Early onset of cortical thinning in children with rolandic epilepsy. NeuroImage Clin 2013; 2: 434–9.

Oyefiade AA, Ameis S, Lerch JP, Rockel C, Szulc KU, Scantlebury N, et al. Development of short-range white matter in healthy children and adolescents. Hum Brain Mapp 2018; 39: 204–17.

Panayiotopoulos CP, Michael M, Sanders S, Valeta T, Koutroumanidis M. Benign childhood focal epilepsies: assessment of established and newly recognized syndromes. Brain 2008; 131: 2264–86.

Pardoe HR, Berg AT, Archer JS, Fulbright RK, Jackson GD. A neurodevelopmental basis for BECTS: evidence from structural MRI. Epilepsy Res 2013; 105: 133–139.

Scholz J, Tomassini V, Johansen-Berg H. Chapter 14—individual differences in white matter microstructure in the healthy brain. In: Johansen-Berg H, Behrens TEJ, editors. Diffusion MRI: from quantitative measurement to in vivo neuroanatomy. 2nd edn. Oxford: Academic Press; 2013. p. 301–16.

Tamnes CK, Østby Y, Fjell AM, Westlye LT, Due-Tønnessen P, Walhovd KB. Brain maturation in adolescence and young adulthood: regional age-related changes in cortical thickness and white matter volume and microstructure. Cereb Cortex 2010; 20: 534–48.

Vadlamudi L, Kjeldsen MJ, Corey LA, Solaas MH, Friis ML, Pellock JM, et al. Analyzing the etiology of benign rolandic epilepsy: a multicenter twin collaboration. Epilepsia 2006; 47: 550–5.

Vadlamudi L, Milne RL, Lawrence K, Heron SE, Eckhaus J, Keay D, et al. Genetics of epilepsy: the testimony of twins in the molecular era. Neurology 2014; 83: 1042–8.

van Mierlo P, Papadopoulou M, Carrette E, Boon P, Vandenberghe S, Vonck K, et al. Functional brain connectivity from EEG in epilepsy: seizure prediction and epileptogenic focus localization. Prog Neurobiol 2014; 121: 19–35.

Vannest J, Tenney JR, Gelineau-Morel R, Maloney T, Glauser TA. Cognitive and behavioral outcomes in benign childhood epilepsy with centrotemporal spikes. Epilepsy Behav 2015; 45: 85–91.

Wickens S, Bowden SC, D'Souza W. Cognitive functioning in children with self-limited epilepsy with centrotemporal spikes: a systematic review and meta-analysis. Epilepsia 2017; 58: 1673–85.

Widjaja E, Skocic J, Go C, Snead OC, Mabbott D, Smith ML. Abnormal white matter correlates with neuropsychological impairment in children with localization-related epilepsy. Epilepsia 2013; 54: 1065–73.

Wierenga LM, van den Heuvel MP, van Dijk S, Rijks Y, de Reus MA, Durston S. The development of brain network architecture. Hum Brain Mapp 2016; 37: 717–29.

Xiao F, An D, Lei D, Li L, Chen S, Wu X, et al. Real-time effects of centrotemporal spikes on cognition in rolandic epilepsy: an EEG-fMRI study. Neurology 2016; 86: 544–51.

Xiao F, Chen Q, Yu X, Tang Y, Luo C, Fang J, et al. Hemispheric lateralization of microstructural white matter abnormalities in children with active benign childhood epilepsy with centrotemporal spikes (BECTS): a preliminary DTI study. J Neurol Sci 2014; 336: 171–79.

Zhang T, Chen H, Guo L, Li K, Li L, Zhang S, et al. Characterization of U-shape streamline fibers: methods and applications. Med Image Anal 2014; 18: 795–807.